COMPUTER METHODS AND PROGRAMS IN BIOMEDICINE XXX (2012) XXX–XXX

journal homepage: www.intl.elsevierhealth.com/journals/cmpb

# Dual transmission model and related spectral content of the fetal heart sounds

*Stephen A. Zahorian*[a,*], *Allan J. Zuckerwar*[b,1,2], *Montri Karnjanadecha*[c,3,4]

[a] *Department of Electrical and Computer Engineering, Binghamton University, Binghamton, NY 13902, United States*
[b] *NASA Langley Research Center, Mail Stop 238, Hampton, VA 23681, United States*
[c] *Department of Computer Engineering, Faculty of Engineering, Prince of Songkla University, Hat Yai, Songkhla 90112, Thailand*

ARTICLE INFO

*Article history:*
Received 22 July 2010
Received in revised form
24 June 2011
Accepted 12 December 2011

*Keywords:*
Fetal phonocardiography
Fetal heart monitoring
Heart sound modeling
Dual transmission model
Digital signal processing

ABSTRACT

A dual transmission model of the fetal heart sounds is presented in which the properties of the signals received on a sensor, installed on the maternal abdominal surface, depend upon the position of the fetus. For a fetus in the occiput anterior position, the predominant spectral content lies in the frequency band 16–50 Hz ("impact" mode), but for a fetus in the occiput posterior position, it lies in the frequency band 80–110 Hz ("acoustic" mode). Signal processing comprises digital bandpass filtering, matched filtering, Teager energy operator, autocorrelation, and figure of merit algorithms. The digital filter permits the user to select the frequency band that best conforms to the prevailing signal mode. Clinical tests on twelve patients, with some in the occiput anterior and some in the occiput posterior fetal positions, support the validity of the dual transmission model.



## 1. Introduction

The fact that the fetal heart sounds are oftentimes difficult to measure reliably is well documented in the literature. The weak pressure signals generated by the fetal heart beat, as detected on the maternal abdominal surface, are contaminated by a variety of effects like fetal movements and breathing [1–3], uterine contractions [2], soufflé [2,3], external noise [3], and impedance mismatch between tissue and transducer [1,4], to name a few. Kovacs et al. [2] point out that the "fetal signal depends on the position of the fetus." Based on this observation, we describe a model whereby the prevailing transmission path of the fetal heart signals to a surface sensor is defined by the fetal position.

## 2. The dual transmission model

Fig. 1 shows a typical spectrum of the fetal heart sounds. For this spectrum, a high pass filter was not used. However, as mentioned later, a high pass analog filter was used in the fetal heart rate system to reduce the expected frequency components below 20 Hz from the maternal heart beat. The prominent peaks in the vicinity of 20 Hz (Region I) are followed by less prominent (lower amplitude) spectral details starting at

* *Corresponding author*. Tel.: +1 607 777 4846.
E-mail addresses: zahorian@binghamton.edu (S.A. Zahorian), ajzuckerwar@yahoo.com (A.J. Zuckerwar), montri@coe.psu.ac.th (M. Karnjanadecha).
[1] Tel.: +1 757 864 4658.
[2] Retired.
[3] Tel.: +66 74 287357.
[4] Visiting research professor at Binghamton University 2010–2011.

0169-2607/$ – see front matter © 2011 Elsevier Ireland Ltd. All rights reserved.
doi:10.1016/j.cmpb.2011.12.006

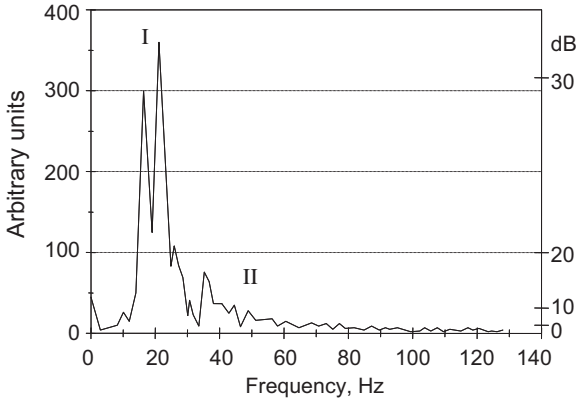


**Fig. 1 – Power spectral density of a typical fetal heart sound, primarily in the impact mode. A linear scale is on the left; a decibel scale is on the right (0 dB = 10 arbitrary units). Region I indicates the impact mode and Region II the acoustic mode (see text).**

about 35 Hz (Region II). In the model proposed here the prominence of each spectral region depends upon the position of the fetus. In particular, according to the model proposed here, the heart sounds depicted in Fig. 1 correspond primarily to one mode; for cases where the second mode is the primary mode, the higher frequency components are more prominent than the lower frequency components. These two modes are described in more detail later. Examples of signals corresponding to the two modes are also given.

Fig. 2 shows a fetus in the occiput anterior position. The fetal back or shoulder is in contact with the maternal abdominal surface directly opposite a sensor. The fetal heart beat generates motion of the entire fetal body, which excites the sensor almost instantaneously by impact. This mode of operation is called here the "impact" mode, having prominent frequency content in the vicinity of 20 Hz, and does not involve acoustical propagation.

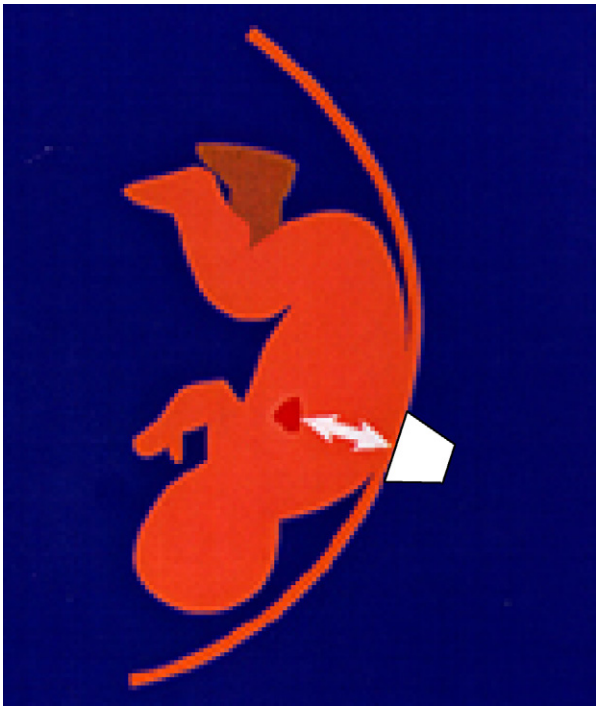

**Fig. 2 – Fetus in the occiput anterior position. A sensor (white) is located directly opposite the fetal contact area on the maternal abdominal surface.**

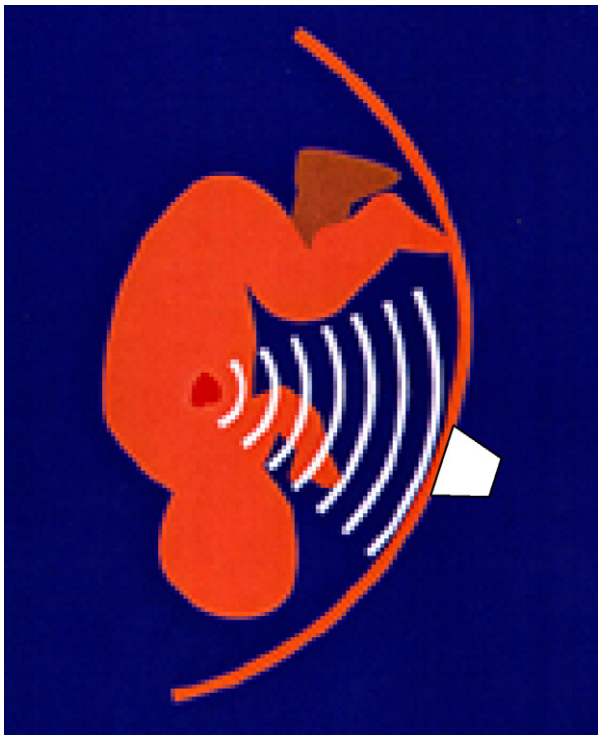

**Fig. 3 – Fetus in the occiput posterior position. A sensor (white) receives fetal heart sounds by means of acoustical propagation across the amniotic fluid.**

Fig. 3 shows a fetus in the occiput posterior position. The fetus makes little contact, if any, with the maternal abdominal surface. The fetal heart, as a pulsating body, generates an acoustical signal which propagates through the amniotic fluid at the speed of sound to the surface sensor. Since the acoustic radiation pressure increases with frequency, the signal is best detected at a frequency higher than that of the impact mode. A frequency band of 80–110 Hz is found to be a good choice; signal detection in a higher frequency band offers no advantage. This mode is called here the "acoustic" mode. The signals in the impact mode are much stronger than those in the acoustic mode.

The impact and acoustic spectral regions are further subdivided into the bands shown in Table 1 to improve the signal-to-noise ratio (SNR). This is especially important for the

**Table 1 – Filter settings selectable by the user.**

| Mode | Filter bands (Hz) |
|---|---|
| Impact | 16–50, 20–50, 20–100 |
| Acoustic | 80–110, 110–160, 160–250, 250–400 |
| Broadband | 20–400, 80–400, none (analog only) |

Please cite this article in press as: S.A. Zahorian, et al., Dual transmission model and related spectral content of the fetal heart sounds, Comput. Methods Programs Biomed. (2012), doi:10.1016/j.cmpb.2011.12.006

acoustic mode because of the weak signal, as is characteristic of a small source radiating at long wavelengths [5].

## 3. Signal processing

This section describes the digital signal processing components of the fetal heart monitoring (FHM) system, which was designed, fabricated, and experimentally evaluated in-house. The signal processing is applied to the electrical signal generated by the sensor installed on the maternal abdominal surface, subsequently amplified and filtered as described in [6]. The primary modifications to the electronics as described in [6] were to replace the front end amplifiers by charge controlled amplifiers and to provide two switch selectable 8th order Butterworth bandpass filter settings—20–400 Hz, and 80–400 Hz. These bandpass filter ranges are based on the model that the lower frequency range would be suited to the occiput anterior position (impact mode) and the higher frequency range more suitable for the occiput posterior position (acoustic mode). Note that since the primary frequency components from the maternal heartbeat were found to be in the 8–15 Hz range, for both of these bandpass filter settings, the maternal heartbeat frequencies were largely filtered out. Note that the two analog bandpass filter ranges were further reduced by digital bandpass filters (16–50 Hz for the impact mode, and 80–110 Hz for the acoustic mode) in order to improve the signal-to-noise ratio. Other filter settings (see Table 1) were tried, but the settings mentioned in the previous sentence seemed to be best overall for the two modes.

Several papers in the literature discuss basic issues in signal processing of fetal signals, including both those obtained from passive listening and those obtained from ultrasound [7–12]. In an early study [7], the authors process signals obtained from a passive acoustic sensor, with a series of filters and autocorrelation methods to identify “first” and “second” heart sounds. In a more recent study [3], the authors describe signal processing with a two channel phonocardiogram to achieve 83% fetal heart rate (FHR) accuracy as compared to fetal heart rate obtained with ultrasound methods. Several investigators (for example [8,9]) have pointed out the difficulty of fetal heart rate detection even with ultrasound (by far the most common method), and compare fetal heart rate obtained with ultrasound with that obtained with direct ECG cardiotocography (the “gold” standard). With some signal processing refinements the correlation between the two methods improves. Other investigators have pointed some problems in assessing variability of FHR due to excessive smoothing of the FHR, generally related to autocorrelation type processing, and have introduced methods to overcome some of these limitations. References [10,11] are representative papers of this type.

The signal processing components are as follows: sampling of the acoustical signal, digital bandpass filtering, matched filtering, Teager energy operator, autocorrelation, and figure of merit. See Fig. 4. All processing for the FHM is performed using overlapping frames of data, with a typical frame length of 6 s (6000 points) and frame advance of 1 s. The frame length is long enough to include 9 fetal heart beats at the relatively low rate of 90 beats per minute (BPM). The frame advance results in the calculation of the FHR 60 times per minute. Some portions of the processing, such as calculation of the matched filter coefficients (Section 3.2), and the figure of merit calculations (Section 3.5) involve multiple frames. Although early versions of the FHM were coded in assembly language using a dedicated DSP board, the version used for the results presented in this paper is coded in C and implemented on an ordinary laptop (virtually any Windows based computer with at least a 1.0 GHz clock speed).

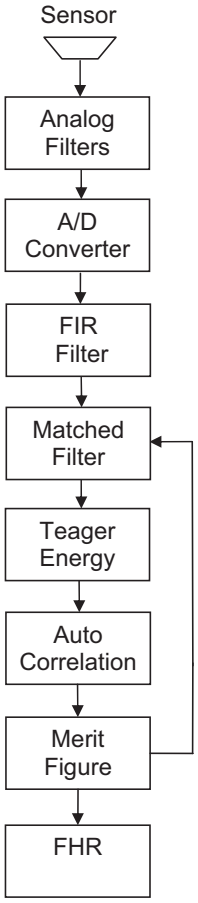


**Fig. 4 – Signal processing flow chart.**

### 3.1. *Sampling and bandpass filtering*

To minimize possibilities for aliasing, the sampling rate used for the first stages of FHM processing is 1000 samples per second. After sampling, the signals are filtered by a 124th order equi-ripple digital bandpass finite impulse response (FIR) linear phase filter. Several filter settings, as shown in Table 1, are available through a menu command. These selections are based on the expectation that the lower ranges would be more suitable for the impact mode, and the higher ranges more suitable for the acoustic mode. The bandpass filter increases the effective SNR of the fetal heartbeats by primarily passing the frequencies in the fetal heart beat, and greatly reducing other acoustical signals such as the maternal heart beat.

Please cite this article in press as: S.A. Zahorian, et al., Dual transmission model and related spectral content of the fetal heart sounds, Comput. Methods Programs Biomed. (2012), doi:10.1016/j.cmpb.2011.12.006

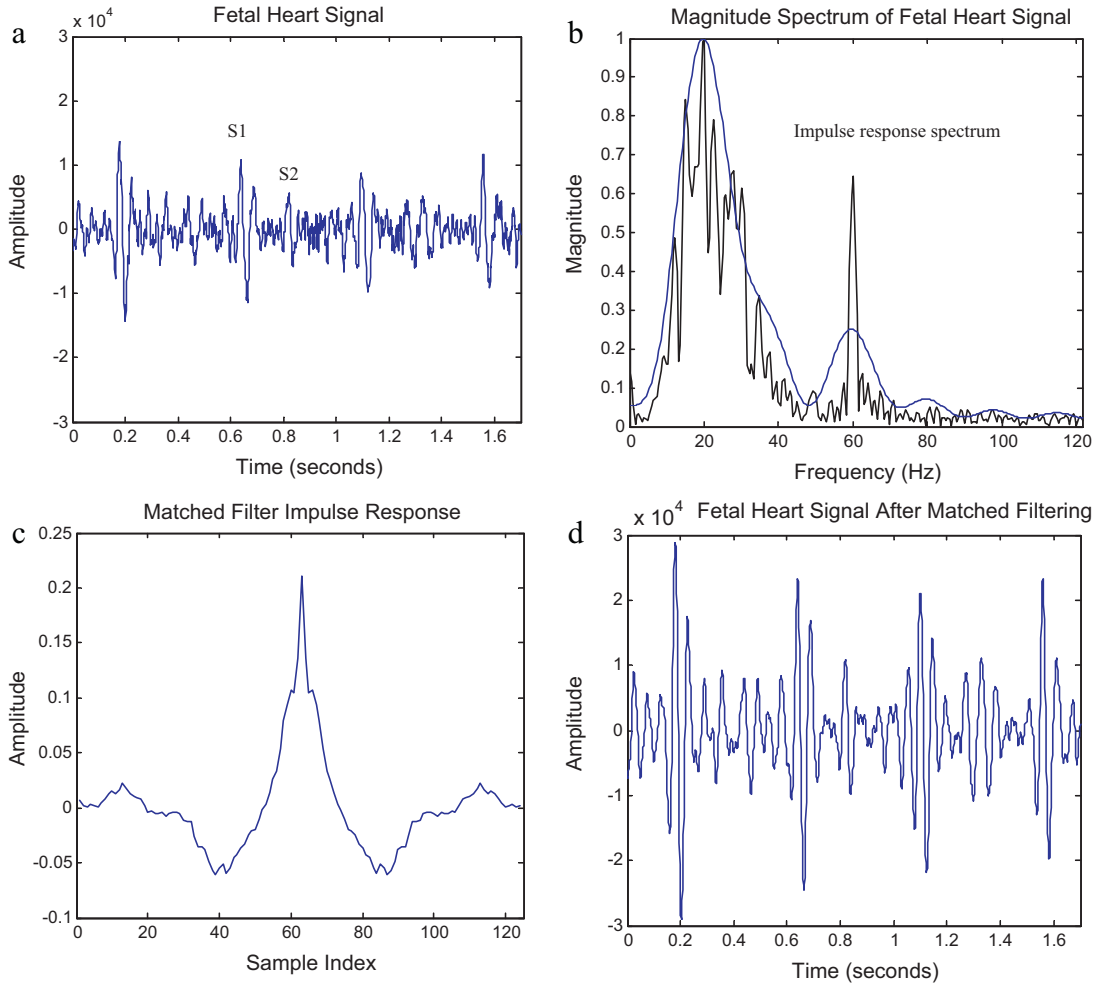


**Fig. 5 – Illustration of matched filtering. Panel (a): Fetal heart signal. Panel (b): Magnitude spectrum of fetal heart signal and impulse response spectrum. Panel (c): Matched filter impulse response. Panel (d): Fetal heart signal after matched filtering.**

### 3.2. *Matched filtering*

Despite the bandpass filtering mentioned above, there is still a great likelihood that the filtered fetal signal contains unwanted components—noise to the FHM. Matched filtering is a technique commonly used to detect recurring time signals corrupted by noise. It has previously been used for fetal heart rate detection [12]. The underlying assumption in matched filtering is that the time signal has a known wave shape. Matched filtering then maximizes the SNR at the output by enhancing this known signal while suppressing the noise. The matched filter is typically represented as a FIR filter. The equation for a FIR filter of order $N$ is given below:

$$y(n) = \sum_{k=0}^{N-1} \hat{h}(k) \times x(n-k) \quad (1)$$

In Eq. (1), the $\hat{h}(k)$ are the matched filter coefficients which ideally correspond to a time-reversed version of the wave shape of the input signal. The $x(n)$ are the samples from the fetal heart signal and the $y(n)$ are the enhanced fetal heart signal (i.e., the output of the filter).

Because the actual wave shape of the fetal heart signal is not known, estimation of the wave shape of the fetal heart signal is necessary. This estimation problem is solved using frequency domain techniques. In particular, a distinctive magnitude spectrum is apparent for "good" sections of the fetal heart signal. This pattern is shown in panel (b) of Fig. 5. As is well known from Fourier and signal processing theory, the envelope of this pattern represents the transform of the basic wave shape, whereas the fine details are related to the periodic nature of the signal. Therefore a good estimate of the time domain waveform corresponding to the fetal heart tone can be obtained from the low-ordered terms in an inverse fast Fourier transform (IFFT) of this magnitude spectrum. This method was used here, but is not explained in detail, since matched filtering is already well described in [12] and since, in the work reported here, it made only a small difference to fetal heart rate tracking accuracy.

To briefly illustrate the steps involved in the matched filtering, Fig. 5 depicts several relevant waveforms. In panel (a) of Fig. 5, a "good" frame of the fetal heart signal is shown. Panel (b) shows the detailed fetal magnitude spectrum (jagged line) and average fetal magnitude spectrum (smooth line). The matched filter coefficients (i.e., matched filter impulse

Please cite this article in press as: S.A. Zahorian, et al., Dual transmission model and related spectral content of the fetal heart sounds, Comput. Methods Programs Biomed. (2012), doi:10.1016/j.cmpb.2011.12.006

response) are displayed in panel (c). Panel (d) shows the fetal heart signal after matched filtering. Note that an arbitrary, but fixed gain, was used with the matched filter. Thus it cannot be inferred that the matched filter itself increases signal amplitude, as might be implied by Fig. 5. The spectrum of $\hat{h}(k)$, which is shown as the "smooth" line in panel (b), is a good match to the envelope of the spectrum of the fetal heart signal. Thus the matched filter coefficients, $\hat{h}(k)$, represent the approximate fetal heart beat pulse shape. Note that this matching is only approximate, because of the estimation process and the lack of use of phase information. However, in off-line experiments with pre-recorded data, the difficult phase estimation step did not result in much improvement. Therefore the implemented matched filter is designed only to match in terms of the magnitude spectrum.

### 3.3. *Teager energy operator*

In order to make the best estimate of fetal heart rate, it is important to identify or emphasize the individual fetal heart beats. The fetal heart beats are seen as areas of local high energy in the fetal heart signal (for example, see panel (a) of Fig. 5). A non-linear operator designed to enhance areas of local high energy is the Teager energy operator proposed by Kaiser [13]. The following equation is used to describe the Teager energy operator:

$$E(n) = s^2(n) - \{s(n-1) \times s(n+1)\}, \quad (2)$$

where $E(n)$ represents a measure of the Teager energy at time $n$. $s(n)$, $s(n+1)$, and $s(n-1)$ are the values of the signal being processed at times $n$, $n+1$, and $n-1$, respectively. When $s(n)$ is greater than $s(n-1)$ and $s(n+1)$ the Teager energy operator will give a large output relative to the signals $s(n-1)$ and $s(n+1)$. A problem with using the Teager energy operator is that noise bursts are enhanced along with the fetal heart tones. However, by combining the Teager energy with matched filtering, as just described, and with autocorrelation calculations, as described in the next section, the fetal heart beats can be enhanced and the noise reduced. Panel (a) of Fig. 6 displays the Teager energy signal computed from a fetal signal. The Teager signal is down sampled by a factor of four, to 250 samples per second, prior to the autocorrelation calculations described in the next section. This reduces the computational time for the autocorrelation, while still providing a potential temporal resolution of 4 ms for final heart rate calculations.

### 3.4. *Autocorrelation*

In order to determine the period of noisy semi-periodic signals, autocorrelation techniques are commonly used. Autocorrelation emphasizes the periodic components in the fetal heart signal while reducing the non-periodic components. This method works provided that the period of the input signal is approximately stationary over the period of the calculation. A frame length of 6 s is typical for the FHM system and is short

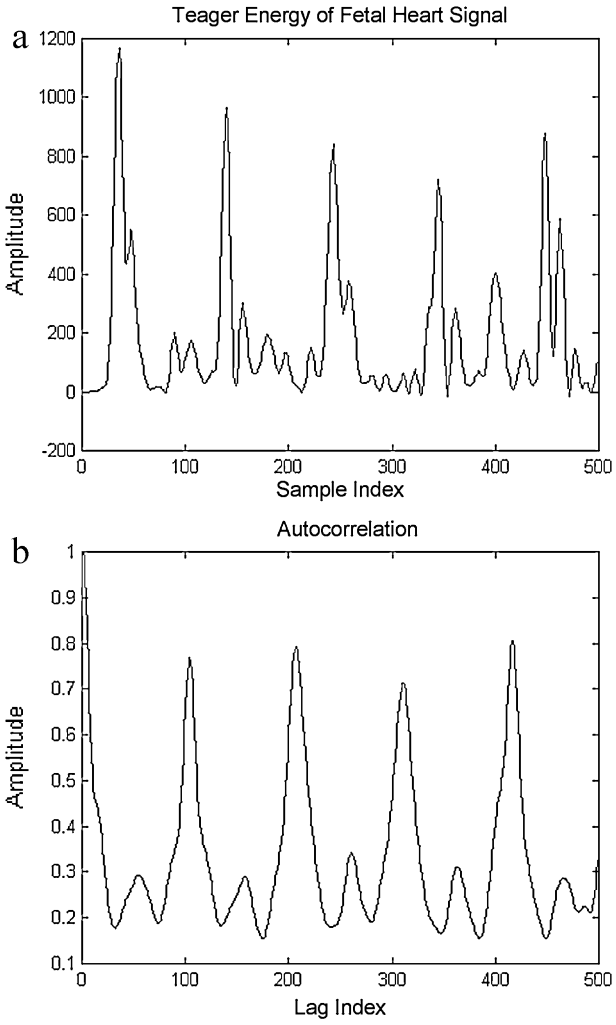


**Fig. 6 – Teager energy signal and autocorrelation. Panel (a): Teager energy signal computed from a fetal heart signal. Panel (b): Autocorrelation signal computed from the Teager energy signal of Panel (a).**

enough that the period of the signal is generally stationary. The autocorrelation is computed as follows:

$$R_a(k) = \sum_{n=0}^{N-k-1} E(n) \times E(n+k), \quad (3)$$

where $E(n)$ is the signal to be processed and $R_a(k)$ is the autocorrelation result. In Eq. (3), $N$ is the frame length and $k$ is the time shift (commonly also called lag index). The autocorrelation depends on time differences only, and not time itself. For typical fetal heart tones the longest expected period is 0.67 s which corresponds to 90 BPM. For slowly varying fetal heart rates, a long autocorrelation window is desired for optimal tracking of the fetal heart rates. On the other hand, rapidly varying fetal heart rates should be computed with a short autocorrelation length. In this work, although an adjustable frame length (increasing the frame length for slow varying heart rates and decreasing the frame length for accelerations and decelerations in the heart rate) was investigated using

Please cite this article in press as: S.A. Zahorian, et al., Dual transmission model and related spectral content of the fetal heart sounds, Comput. Methods Programs Biomed. (2012), doi:10.1016/j.cmpb.2011.12.006

**Table 2 – Summary of patient data acquired from low-frequency LF (16–50 Hz) and high-frequency HF (80–110 Hz) bands during non-stress tests (NST).**

| Patient | LF energy ($mV^2$) | HF energy ($mV^2$) | Freq. band of NST | Fetal position[a,b] |
|---|---|---|---|---|
| 1 | 841 | 16 | LF | A |
| 2 | 19,044 | 2500 | LF | A |
| 3 | 4356 | 361 | LF | A |
| 4 | 41,209 | 484 | LF | A |
| 5 | No data: merit figure below threshold | | | |
| 6 | 81 | 1225 | Hf | P |
| 7a[c] | 85 | 773 | HF | P |
| 7b | 6100 | 36 | LF | A |
| 8 | 1296 | 7921 | HF | P |
| 9 | 729 | 6724 | HF | P |
| 10 | 529 | 8464 | HF | P |
| 11 | No data: merit figure below threshold | | | |
| 12 | 17,689 | 400 | LF | A |

[a] Fetal positions determined independently by palpitation, except for patients 8 and 10, for which ultrasonic imaging was employed.
[b] A = occiput anterior position; P = occiput posterior position.
[c] For the first 9 min, the HF band was used for the NST; from 9 min to the end the LF band was used. It is believed that the fetus changed position during the NST.

recorded signals, for the final real-time implementation, a fixed frame length of 6 s is used. For periodic signals, $R_a(k)$ is maximum if $k$ is equal to a multiple of the period. If the fetal signals were the only periodic source, autocorrelation alone could be used to determine the fetal heart rates. However, periodic noise does corrupt the fetal heart signal leading to peaks in the autocorrelation result that do not correspond to the FHR. The fetal heart rates, in beats per minute, are calculated from peaks in the autocorrelation as follows:

$$\mathrm{FHR} = \frac{Fs \times 60}{k}, \tag{4}$$

where $Fs$ is the effective sampling frequency (250 Hz) and $k$ is the lag index of the autocorrelation peak. Additional processing, using the figure of merit as described in the next section, is used to separate FHR peaks from spurious peaks. Panel (b) of Fig. 6 shows the autocorrelation signal computed from the Teager energy signal of panel (a). For this autocorrelation, the first major peak in the autocorrelation occurs at a lag index of approximately 105, implying the FHR would be about 143 BPM.

### 3.5. *Figure of merit*

A figure of merit is calculated for each heart rate corresponding to each peak in the autocorrelation signal. The figure of merit is used to determine the best heart rate from many heart rate candidates. The higher the value of the figure of merit the more confidence there is in the corresponding heart rate. There are two primary factors that contribute to the figure of merit. The first factor is the size of the peak in the autocorrelation result. The second factor of the figure of merit is the deviation of the rate candidate from the average heart rate. The average heart rate is a weighted combination of previously detected heart rates:

$$\overline{\mathrm{Rate}} = \sum_{i=1}^{N_R} \mathrm{Rate}(i) \times \mathrm{Merit}(i), \tag{5}$$

where the weighting factor is the merit (but first normalized so that the sum of the merits over the averaging interval is 1.0) of each heart rate. The merit calculation combines the two factors mentioned above into one equation:

$$\mathrm{Merit} = \frac{R_a(k)}{R_a(0)} \left( 1.0 - \overline{\mathrm{Merit}} \times \frac{\left| \mathrm{Rate} - \overline{\mathrm{Rate}} \right|}{\sigma_R} \right), \tag{6}$$

where $\sigma_R$ is the rate deviation, $R_a(k)$ is the autocorrelation value, and $R_a(0)$ is the energy of the signal which normalizes the autocorrelation values between 0 and 1. Note that the rate deviation $\sigma_R$ is empirically set to 50 BPM, as opposed to the actual standard deviation of the FHR. Although in principle Merit could be negative, in practice, for this value of $\sigma_R$, this was never found to be the case for the highest merit candidate in each frame. The average merit ($\overline{\mathrm{Merit}}$) and average heart rate is typically calculated over the previous five merits and heart rates. To determine the reliability of the final detected heart rate, a threshold is used. If the figure of merit for the final detected heart rate is above the nominal threshold, then the FHM system has "confidence" in the FHR. Conversely, if the figure of merit is below the threshold then the heart rate is considered unreliable, and called a "drop-out." The threshold is set typically at a value of 0.45 out of a maximum set arbitrarily at 0.95. This value of 0.45 was set empirically; with this threshold, most of the "confident" fetal heart rate traces were found to correspond closely to simultaneously recorded ultrasound fetal traces, whereas with a lower merit threshold there was poorer correspondence between the fetal heart traces obtained with the methods described in this paper and the ultrasound obtained traces, for the low merit regions.

## 4. Results

The hardware described in [6] was used to determine the following acoustical time histories and fetal heart rate records. Panel (a) of Fig. 7 shows a two-second snapshot of the

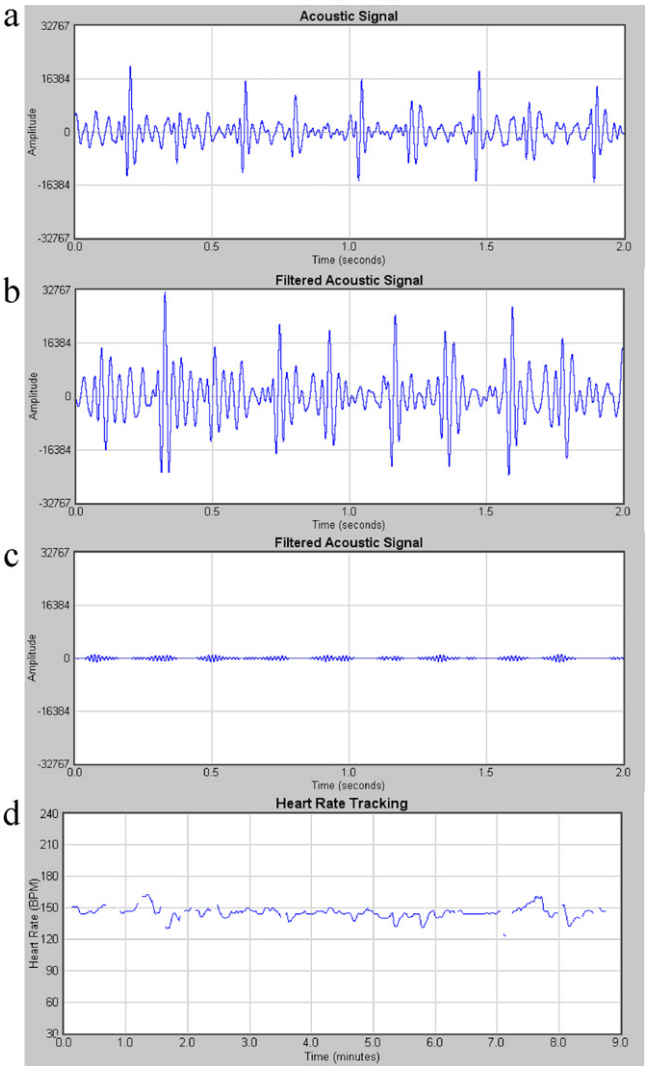


**Fig. 7 – Acoustical signal of fetus in the occiput anterior position. Panel (a): 2-s snapshot of the original signal. Amplitude scale is arbitrary. Panel (b): 2-s snapshot of the signal after filtering with a pass band 16–50 Hz. Amplitude scale same as above. Panel (c): 2-s snapshot of the signal after filtering in pass band 80–110 Hz. Amplitude scale same as above. Panel (d): 9-min record of the fetal heart rate (pass band 16–50 Hz).**

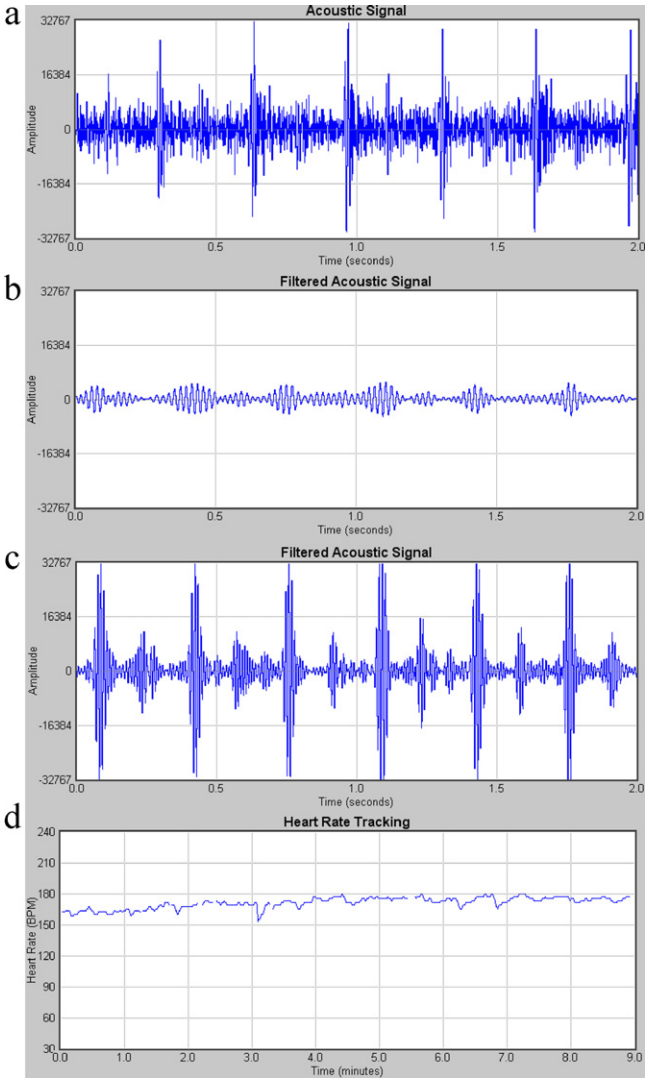


**Fig. 8 – Acoustical signal of fetus in the occiput posterior position. Panel (a): 2-s snapshot of the original signal. Amplitude scale is arbitrary. Panel (b): 2-s snapshot of the signal after filtering with a pass band 16–50 Hz. Amplitude scale same as above. Panel (c): 2-s snapshot of the signal after filtering with a pass band 80–110 Hz. Amplitude scale same as above. Panel (d): 9-min record of the fetal heart rate (pass band 80–110 Hz).**

acoustical time history of an occiput anterior patient. Panel (b) of Fig. 7 shows the same snapshot of the acoustical time history as in panel (a), at the same vertical scale, but within the frequency band 16–50 Hz. The first and second heart sounds are clearly discernable. The acoustical signal is but little contaminated by noise, the merit figure being 0.95. Panel (c) of Fig. 7 shows the same snapshot of the acoustical time history as in panel (a), but within the frequency band 80–110 Hz. The latter signal is too attenuated to be useful for measuring the fetal heart rate. These records suggest that the transmission path corresponds to the impact mode. Panel (d) of Fig. 7 shows a 9-min record of the fetal heart rate measured within the 16–50 Hz frequency band.

In Fig. 8, panel (a) shows a 2-s snapshot of the acoustical time history of an occiput posterior patient and panel (b) shows the same 2-s snapshot, at the same vertical scale, in the frequency band 16–50 Hz. In this case the impact mode is suppressed, and the only opportunity for the fetal heart signal to reach the surface sensor is by means of the acoustic mode. Panel (c) of Fig. 8 shows the same snapshot of the acoustic signal as in panel (a), but within the frequency band 80–110 Hz, and as before, the first and second heart sounds are clearly discernable, the merit figure remaining at 0.95. Panel (d) of Fig. 8 shows a 9-min record of the fetal heart rate taken within the 80–110 Hz frequency band.

Out of a population of 12 test subjects at Eastern Virginia Medical School, three were found to conform to the

Please cite this article in press as: S.A. Zahorian, et al., Dual transmission model and related spectral content of the fetal heart sounds, Comput. Methods Programs Biomed. (2012), doi:10.1016/j.cmpb.2011.12.006

"impact" mode, four to the "acoustic" mode, three to both modes (patients 3, 4, and 7) and two were found to yield no useful result. For the case of patient 7, the fetus appeared to first be in the occiput posterior position ("acoustic" mode), but later changed position to the occiput anterior position ("impact") mode. The mode was selected based on higher average figure of merit. The fetal position was also determined independently by palpitation or in some cases by ultrasonic imaging. For all patients except 3, 4, and 7, for whom the fetal position was indeterminate, the fetal position matched that predicted by the model presented in this paper. Table 2 summarizes the data for these 12 subjects, in terms of low frequency (LF) energy and high frequency (HF) energy, after analog filtering. For the LF cases the recorded signals still contained both the low and high frequency signals, but clearly the LF energy was much greater than the HF energy. For the HF cases, most of the low frequency energy was removed, and good FHR traces (by comparison with the ultrasound traces, obtained immediately prior) were obtained from the HF energy. The fetal phonocardiographic tests were conducted after scheduled ultrasonic non-stress tests.

## 5. Conclusions

The dual transmission model of the fetal heart tone and the effectiveness of the associated signal processing algorithms have been supported by a few preliminary clinical tests, briefly summarized in Table 2. For the case of a fetus in the occiput anterior position, the primary spectral content of the fetal heart sounds was found to lie in the 16–50 Hz pass band (impact mode). For the case of a fetus in the occiput posterior position, the primary spectral content was found to lie in the 80–110 Hz pass band (acoustic mode). The results obtained from limited clinical testing are consistent with the model. Consequently, knowledge of the fetal position and selection of the appropriate pass band are essential for effective measurement of the fetal heart sounds. The limited number of clinical patients (12) used in this study is too small to clearly infer the clinical applications of the proposed model and signal processing methods. However, the preliminary clinical data supports the dual transmission model.

## Conflict of interest statement

The authors have no conflicts of interest to declare.

## Acknowledgements

The authors gratefully acknowledge the work of Timothy Bryant, Nancy Holloway, and Dennis Mowrey, NASA Langley Research Center, for fabricating the fetal heart rate monitor used in this study. The authors further thank the following persons for assistance in conducting the fetal heart monitoring tests: Dr. Margarita De Veciana, MD, and Linda Bennington, RN, of the Fetal Diagnostic Unit, Eastern Virginia Medical School, Norfolk, VA, and Dr. Micki L. Cabaniss, MD, Western Carolina Maternal-Fetal Medicine, Asheville, NC. The test protocol was approved by the institutional review boards of NASA Langley Research Center, Old Dominion University, Eastern Virginia Medical School, and Western Carolina Maternal-Fetal Medicine. Financial support was provided by the Technology Utilization Office of NASA Langley Research Center.

## REFERENCES

[1] D.G. Talbert, W.L. Davies, F. Johnson, N. Abraham, N. Colley, D.P. Southall, Wide bandwidth fetal phonography using a sensor matched to the compliance of the mother's abdominal wall, IEEE Trans. Biomed. Eng. SMB-33 (1986) 175–181.
[2] F. Kovacs, M. Torok, I. Habermajer, A rule-based phonocardiographic method for long-term fetal heart rate monitoring, IEEE Trans. Biomed. Eng. 47 (2000) 124–130.
[3] P. Varady, L. Wildt, Z. Benyo, A. Hein, An advanced method in fetal phonocardiography, Comput. Methods Programs Biomed. (Elsevier) 71 (3) (2003) 283–296.
[4] J. Nagel, New diagnostic and technical aspects of fetal phonocardiography, Eur. J. Obstet. Gynocol. Reprod. Biol. 23 (1986) 295–303.
[5] P.M. Morse, K.U. Ingard, Theoretical Acoustics, McGraw-Hill, New York, 1968.
[6] A.J. Zuckerwar, R.A. Pretlow, J.W. Stoughton, D.A. Baker, Development of a piezopolymer pressure sensor for a portable fetal heart rate monitor, IEEE Trans. Biomed. Eng. 40 (1993) 963–969.
[7] J.T.E. McDonnell, J. Dripps, P. Grant, Processing and analysis of fetal phonocardiograms, in: Proc. Annu. Int. Conf. IEEE Eng. in Medicine and Biology Society, vol. 11, 1989, pp. 61–62.
[8] C.H.L. Peters, E.D.M. ten Broeke, P. Andriessen, B. Vermeulen, R.C.M. Berendsen, P.F.F. Wijn, S.G. Oei, Beat-to-beat detection of fetal heart rate: Doppler ultrasound cardiotocography compared to direct ECG cardiotocography in time and frequency domain, Physiol. Meas. 25 (2004) 585–593.
[9] H. Cao, D.E. Lake, J.E. Ferguson II, C.A. Chisholm, M.P. Griffin, J.R. Moorman, Toward quantitative fetal heart rate monitoring, IEEE Trans. Biomed. Eng. 53 (2006) 111–118.
[10] J. Jezewski, T. Kupka, K. Horoba, Extraction of fetal heart-rate signal as the time event series from evenly sampled data acquired using Doppler ultrasound technique, IEEE Trans. Biomed. Eng. 55 (2) (2008) 805–810.
[11] J. Wrobel, J. Jezewski, D. Roj, T. Przybyla, R. Czabanski, A. Matonia, The influence of Doppler ultrasound signal processing techniques on fetal heart rate variability measurements, Int. J. Biol. Biomed. Eng. 4 (4) (2010) 79–87.
[12] M. Ruffo, M. Cesarelli, M. Romano, P. Bifulco, A. Fratini, An algorithm for FHR estimation from foetal phonocardiograpic signals, Biomed. Signal Process. Contr. 5 (2) (2010) 131–141.
[13] J.F. Kaiser, On a simple algorithm to calculate the 'energy of a signal', in: Proc. IEEE Int. Conf. on Acoustics, Speech and Signal Processing (ICASSP-90), 1990, pp. 381–384.

Please cite this article in press as: S.A. Zahorian, et al., Dual transmission model and related spectral content of the fetal heart sounds, Comput. Methods Programs Biomed. (2012), doi:10.1016/j.cmpb.2011.12.006